EXHIBIT A

668 J. Agric. Food Chem. 2010, 58, 668–675
DOI:10.1021/jf902660n

JOURNAL OF AGRICULTURAL AND FOOD CHEMISTRY
ARTICLE

Molecular Mechanism of Hesperetin-7-*O*-glucuronide, the Main Circulating Metabolite of Hesperidin, Involved in Osteoblast Differentiation

ANNA TRZECIAKIEWICZ,[†] VERONIQUE HABAUZIT,[†] SYLVIE MERCIER,[†] DENIS BARRON,[†] MIREIA URPI-SARDA,[†,§] CLAUDINE MANACH,[†] ELIZABETH OFFORD,[‡] AND MARIE-NOELLE HORCAJADA*[,†,‡,∥]

[†]INRA Clermont-Ferrand/Theix, Human Nutrition Unit UMR1019, F-63122 St. Genes Champanelle, France, [‡]Nestle Research Center, Vers-Chez-Les-Blanc, 1000 Lausanne 26, Switzerland, and [§]University of Barcelona, XaRTA, INSA, Pharmacy Faculty, Nutrition and Food Science Department, E-08028 barcelona, Spain. [∥]Current address: Department of Nutrition & Health, Nestlé Research Center, P.O. Box 44, CH-1000 Lausanne 26, Switzerland.

Citrus fruit hesperidin is hydrolyzed by gut microflora into aglycone form (hesperetin) and then conjugated mainly into glucuronides. We previously demonstrated that hesperetin enhanced osteoblast differentiation. In this study, we examined the effect of hesperetin-7-*O*-glucuronide (Hp7G) on primary rat osteoblast proliferation and differentiation. The impact of Hp7G on specific bone signaling pathways was explored. Osteoblasts were exposed to physiological concentrations of 1 (Hp7G1) and 10 (Hp7G10) μM of conjugate. The glucuronide did not affect proliferation but enhanced differentiation by significantly increasing alkaline phosphatase (ALP) activity from day 14 of exposure. Hp7G significantly induced mRNA expression of ALP, Runx2, and Osterix after 48 h of exposure. Moreover, phosphorylation of Smad1/5/8 was enhanced by Hp7G, while ERK1/2 remained unchanged after 48 h. Hp7G decreased RANKL gene expression. These results suggest that Hp7G may regulate osteoblast differentiation through Runx2 and Osterix stimulation, and might be implicated in the regulation of osteoblast/osteoclast communication.

KEYWORDS: Flavonoid metabolite; hesperetin 7-*O*-glucuronide; osteoblast differentiation; Osterix; Runx2

INTRODUCTION

Hesperidin (hesperetin-7-*O*-rutinoside) is a glycoside flavonoid belonging to the flavanone subgroup, found mainly in citrus fruits. When absorbed, hesperidin is hydrolyzed by gut microflora into the aglycone form (hesperetin) and then conjugated by the phase II drug-metabolizing enzymes into glucuronides (87% of total metabolites of hesperetin), sulfates, or sulfoglucuronides (*1*, *2*). In rodents fed 0.5% hesperidin in the diet, the circulating concentrations of aglycone hesperetin ranged from 3.5 to 5.5 μM (*3*, *4*), while 1 μM was measured in humans (*1*). Several biological activities such as antioxidant, anti-inflammatory, analgesic, and lipid lowering effects (*5*) have been attributed to hesperidin and its metabolites. Some authors have shown that hesperidin inhibits bone loss in ovariectomized mice (*3*) or rats (*4*) and prevents bone loss in male orchidectomized rats (*6*). The mechanisms by which hesperidin may affect skeletal metabolism still remain unclear. Nevertheless, it was recently shown that hesperetin may regulate primary rat osteoblast differentiation through bone morphogenetic protein (BMP) signaling (*7*).

The metabolism of flavonoids is similar to that of xenobiotics (*8*). Even if conjugates have been presented as forms of elimination and detoxification, in vitro biological properties of flavonoid conjugates found in vivo were reported (*9*). One reported study tested conjugated forms in osteoblastic cells and demonstrated that quercetin-3-glucuronide was able to increase the bone sialoprotein mRNA level in osteoblast-like ROS 17/2.8 cells (*10*). Only two in vitro studies were performed using hesperetin conjugates such as glucuronides in skin fibroblast cells (*11*) and hesperetin 7-*O*-glucuronide and 5-nitro-hesperetin in cortical neurons (*12*). To date, no effect of hesperetin conjugate on osteoblasts has been reported.

The available studies reporting flavonoid effect on osteoblastic cells have been performed with aglycone compounds. These compounds were able to stimulate ALP activity, which is one of the major osteoblast differentiation markers probably by upregulation of expression of two transcription factors such as Runx2 and Osterix (*13*) strongly implicated in the regulation of osteoblast functions (*14*). Moreover, Runx2 has a central function in coordinating multiple signals including AP-1 (commonly composed of c-Jun/c-fos) and Smad factors, which are involved in osteoblast differentiation (*15*). Runx2 and Osterix also play a role in the BMP pathway that may, in turn, activate different signaling cascades and Smad-dependent and independent pathways, including ERK, JNK, and p38 MAPK (*16*). Within flavonoids, there is also evidence that they are susceptible to the influence of

*Corresponding author. Phone: +41 21 785 8130. Fax: +41 21 785 8925. E-mail: marienoelle.horcajada@rdls.nestle.com.

 Published on Web 11/18/2009

the OPG/RANKL/RANK regulatory triad implicated in the osteoblast and osteoclast relationship (*17*, *18*). Osteoblasts produce both receptor activator of nuclear factor-kappaB (RANK) ligand (RANKL) and osteoprotegerin (OPG). OPG acts as a decoy receptor for RANKL and thereby neutralizes its function in osteoclastogenesis. Bone homeostasis depends on the local RANKL/OPG ratio (*19*).

The aim of this study was to assess the effect of hesperetin conjugate on osteoblast functions and the molecular mechanisms involved. Thus, the influence of hesperetin-7-*O*-glucuronide (Hp7G) at physiologically relevant concentration (1 and 10 μM) was tested in primary rat osteoblasts.

MATERIALS AND METHODS

Synthesis of Hesperetin-7-*O*-glucuronide. Hesperetin 7-*O*-glucuronide (Hp7G) has been chemically prepared by glucuronidation of its suitable precursor using 2,3,4-triacetyl-α-methyl glucurono-pyranosyl-(*N*-phenyl)-2,2,2-trifluoroacetimidate, followed by acetate deprotection using zinc acetate, and methyl ester hydrolysis using Pig Liver Esterase, according to Boumendjel et al. (*20*). The purity of the synthesized molecule examined by HPLC was 100%.

Cell Culture. Primary osteoblasts were isolated from the calvaria of newborn Wistar rats (INRA, Theix, France) by enzymatic digestion as described previously (*21*). Cells were maintained in α-minimal essential medium (α-MEM) (GIBCO, Paisley, UK) with 10% heat-inactivated fetal bovine serum (FBS) and 1% penicillin/streptomycin (GIBCO, Paisley, UK) in 5% CO_2 at 37 °C conditions. Cells were seeded on type I collagen-coated (BD Biosciences, Bedford, USA) 96-well plates at a density of 3500 cells/w, in 60 mm Petri dishes (4×10^5 cells/dish) or in 100 mm Petri dishes (5×10^5 cells/dish), and cultured for 2 days in α-MEM to reach confluence (which correspond to day 0 of cell culture for treatment exposure duration). Cells were then exposed to different conditions: minimal medium (C−), minimal medium containing 50 μg/mL ascorbic acid, 5 mM β-glycerophosphate (C+, optimized medium), and minimal medium supplemented with 1 μM (Hp7G1) or 10 μM (Hp7G10) hesperetin-7-*O*-glucuronide (Hp7G). Hp7G was dissolved in DMSO. In every condition, the final concentration of DMSO in medium was 0.1%. The medium was changed every 2 days. All cell experiments were performed in triplicate.

Cellular Uptake. Eight percent confluent cells were exposed for 24 h to 40 μM hesperetin (Hp), hesperetin-7-*O*-glucuronide (Hp7G), or vehicle (0.1% DMSO). Culture medium was collected after 0, 8, and 24 h of exposition in the presence or absence of cells and extracted with 2.5 volumes MeOH/H_2O (70:30) acidified with 200 mM HCl. After centrifugation (14000 rpm for 4 min), extracts were analyzed by liquid chromatography−tandem mass spectrometry (HPLC-MS/MS). The recovery rate for the extraction of Hp7G and Hp from the culture medium was 86 and 75%, respectively.

After 24 h of exposure, cells were rinsed three times using PBS (Sigma, Steinheim, Germany) then exposed to 0.5 mL of MeOH/H_2O (70:30) acidified with 200 mM HCl and scraped using a cell scraper (BD Falcon, Bedford, USA). These extraction conditions, in particular the small volume of solvent added, were chosen to maximize the concentration of metabolites in the extracts in order to facilitate a qualitative analysis of the metabolite uptake; however, they were not optimized for the quantitative analysis of flavanones in the intracellular medium.

HPLC-MS/MS Analysis. Liquid chromatography (LC) analyses were performed using a Hewlett-Packard 1100 HPLC system (Agilent Technologies, Waldbronn, Germany) equipped with a quaternary pump and an autosampler. An Applied Biosystems API 2000 triple quadrupole mass spectrometer (PE Sciex, Ontario, Canada), equipped with a Turbo IonSpray source ionizing in the negative mode at 550 °C was used. Optimized parameters for the detection of Hp and Hp7G were the following: capillary voltage, −4500 V; collision gas, 5 (arbitrary units); and curtain gas, 30 (arbitrary units). Declustering potential, focusing potential, entrance potential, and collision energy were optimized with infusion experiments of Hp (−50 V, −350 V, −5 V, and −30 V, respectively) and Hp7G (−16 V, −350 V, −10 V, and −26 V, respectively).

A SymmetryShield RP18 column (Waters, Milford, MA, USA), 2.1 × 150 mm i.d., 5 μm, was used for chromatographic separation. Linear gradient elution was performed as follows: 0−20 min 85% A to 100% B, with 0.1% formic acid as mobile phase A and 100% acetonitrile as mobile phase B. The column was re-equilibrated for 10 min. The flow rate was 400 μL/min, and the injection volume was 20 μL.

Data were acquired using the multiple reaction monitoring (MRM) mode, monitoring the Hp transition (301/164) and the Hp7G transition (477/301).

Cell Proliferation. Cell proliferation was measured by determining DNA content on days 0, 5, 9, 14, and 19. Cells were incubated with 2 μg/mL of bisbenzimide H 33342 (Hoechst) in PBS at 37 °C. The total amount of DNA was measured with FLX800 Microplate Fluorescence Reader (Bio-Tek Instruments, Winooski, VT, USA) at 360 nm wavelength (excitation) and 460 nm (emission). Fold increase in cell number was calculated relative to the initial cell number on day 0 (value = 1).

ALP Activity Measurement. Enzymatic activity of alkaline phosphatase (ALP) was measured kinetically on treatment days 0, 5, 9, 14, and 19 according to the method described by Sabokbar et al. (*22*). Osteoblasts were lysed by the freeze−thaw cycle and homogenization into 200 μL of diethanolamine/magnesium chloride hexahydrate buffer at pH 9.8 (Sigma, Steinheim, Germany). Cell lysate (10 μL) was added to 200 μL of *p*-nitrophenyl phosphate solution (Sigma, Steinheim, Germany). Absorbance was measured at 405 nm, 30 °C, and every 2 min 30 s during 30 min using an ELX808 microplate reader (Bio-Tek Instruments, Winooski, VT, USA). ALP activity was expressed as μmol *p*-nitrophenol/hour/mg protein. Protein measurement was performed according to Bradford's method using the BioRad protein assay (BioRad, Munich, Germany).

Real-Time PCR. Upon confluence, cells were exposed to different media: C−, C+, Hp7G1, or Hp7G10 for 24 and 48 h. After 24 and 48 h of treatment, total RNA and proteins were isolated using the NucleoSpin RNA/Protein Kit (Macherey-Nagel, Hoerdt, France). Total RNA concentration and purity were measured with a NanoDrop spectrophotometer (Wilmington, USA). RNA integrity was checked using the RNA 6000 Nano Assay kit with an Agilent 2100 bioanalyzer (Agilent Technologies, Santa Clara, USA). Reverse transcription of RNA was performed using the Ready-To-Go, You-Prime First-Strand Beads Kit (Amersham Biosciences, Piscataway, USA). The SYBR Premix Ex Taq (Perfect Real Time) (TaKaRa, Shiga, Japan) was used to quantify gene expression by Real-Time PCR. The PCR (program, 95 °C-30 s; 40 cycles, 95 °C-5 s; 60 °C-35 s) was performed using Mastercycler bp Realplex (Eppendorf, Hamburg, Germany). Target gene expression was normalized to the housekeeping gene β-actin. The $2^{-\Delta\Delta C_T}$ method was applied to calculate relative gene expression compared to the C− condition, which corresponds to a value of 1 (*23*). The primers used for PCR are listed in Table 1.

Western Blot Analysis. Upon confluence, cells were exposed to different media: C−, C+, Hp7G1, or Hp7G10 for 24 and 48 h. The concentration of proteins isolated using the NucleoSpin RNA/Protein kit (Macherey-Nagel, Hoerdt, France) was measured by a BC assay kit (Uptima Interchim, Montluçon, France). Twenty-five micrograms of total protein was subjected to a 10% SDS−polyacrylamide gel and transferred to Immobilon-P-PVDF membranes at 100 V for 1 h and 45 min. The membranes were blocked in 5% nonfat dry milk in TBS-T (0.5% Tween 20) buffer for 2 h. Blots were incubated with antiphospho-Smad1/5/8 or antiphospho-ERK1/2 (Cell Signaling, Beverly MA, USA) at a 1:1000 dilution for 1 h at room temperature, then probed with 1:2000 diluted antirabbit horseradish peroxidase (HRP) conjugated secondary antibody (Santa Cruz Biotechnology, Santa Cruz, USA) for 1 h at room temperature. The blot signals were detected by enhanced chemiluminescence (ECL Plus, Amersham GE Healthcare, Buckinghamshire, UK). After stripping in a buffer containing 0.7% β-mercaptoethanol, membranes were labeled with 1:500 diluted anti-Smad1/5/8 (Santa Cruz Biotechnology, Santa Cruz, CA, USA) or 1:1000 diluted anti-ERK1/2 (Cell Signaling, Beverly MA, USA) and probed with 1:5000 diluted secondary antibody.

Statistical Analysis. Results are expressed as mean ± SEM. ALP activity and cell proliferation on each day were analyzed using parametric one-way ANOVA, followed by multiple comparisons Fisher/LSD performed in XLSTAT version 7.5.2 (AddinSoft, Paris, France).

Nonparametric test−Wilcoxon signed rank test (compared to control C−; hypothetical median = 1) on GraphPad InStat 3 software (San Diego, CA, USA) was used for statistical analysis of gene expression. p-value < 0.05 was considered statistically significant.

RESULTS

An optimized medium (C+) was used as a positive control of differentiation, and Hp7G was added to minimal medium (C−) to observe its proper action and not in synergy with ascorbic acid.

Cellular Uptake. The cellular uptake of Hp and Hp7G in primary rat osteoblasts was determined by HPLC-MS/MS analysis after 24 h of cell exposure to 40 μM Hp or Hp7G.

The compound stability in the growth medium was followed over 24 h in the presence and absence of cells. No degradation of the aglycone was observed in the absence of cells. In the presence of cells exposed to the aglycone, a peak with the characteristic MS/MS transition of hesperetin−glucuronide (MRM 477/301) was detected in the medium after 8 and 24 h, in concentration increasing with time (**Figure 1**). This peak showed the same retention time (8.19 min) as the standard Hp7G, suggesting that this specific metabolite was produced by the cells exposed to the aglycone. A minor peak also appeared at the same MS/MS transition and slightly higher retention time (8.3 min), and may correspond to the hesperetin-4′-*O*-glucuronide. Glucuronidation must have occurred inside the cells since glucuronidases are not present at the surface of cell membranes.

When cells were exposed for 24 h to hesperetin, Hp but not Hp7G was detected in the cell extract (**Figure 2B**). The intracellular concentration of Hp7G was below the limit of detection (18.5 nmol/L) probably because Hp7G was exported outside the cells by transporters.

When cells were exposed to Hp7G, a small hydrolysis into Hp (0.15%) was observed in the medium after 8 h and slightly increased at 24 h (0.6%) (chromatograms not shown). A small hydrolysis of Hp7G was also observed in the medium after 24 h in

Table 1. Primer Sequences for Real-Time PCR

transcript	primers (5′-3′)	product size
β-actin	forward: AGTGTGACGTTGACATCCGTA	112 bp
	reverse: GCCAGAGCAGTAATCTCCTTCT	
Runx2	forward: CGATCTGAGATTTGTAGGCCG	159 bp
	reverse: TCATCAAGCTTCTGTCTGTGCC	
Osterix	forward: AAGAGGTTCACCCGCTCTGA	122 bp
	reverse: TGATGTTTGCTCAAGTGGTCG	
OPG	forward: GGGCGTTACCTGGAGATCG	125 bp
	reverse: GAGAAGAACCCATCTGGACATTT	
RANKL	forward: GGCCACAGCGCTTCTCAG	143 bp
	reverse: AGTGACTTTATGGGAACCCGAT	
Noggin	forward: CACTATCTACACATCCGCCCAG	110 bp
	reverse: AGCGTCTCGTTCAGATCCTTCT	
BMP2	forward: GCCAGGTGTCTCCAAGAGACAT	179 bp
	reverse: AGCTGGACTTAAGACGCTTCCG	
BMP4	forward: GACTTCGAGGCGACACTTCT	100 bp
	reverse: GCCGGTAAAGATCCCTCATGTA	
Smad1	forward: CCACAACCCTATTTCGTCGGT	102 bp
	reverse: ATCCTGTCTGACTTCTCCGTCC	
Smad5	forward: TGAACTGAACAACCGTGTCGG	151 bp
	reverse: CCTGGTGTTCTCGATGGTTGAG	
c-Jun	forward: CCTCCCGTCTGGTTGTAGGAAT	145 bp
	reverse: CCCTTGCAACACCCTCTTCTTC	
c-fos	forward: TTCACCCTGCCTCTTCTCAATGAC	82 bp
	reverse: GCCTTCAGCTCCATGTTGCTAATG	
ALP	forward: ACAGCCATCCTGTATGGCAA	97 bp
	reverse: GCCTGGTAGTTGTTGTGAGCA	
OPN	forward: AGCAAGAAACTCTTCCAAGCAA	129 bp
	reverse: GTGAGATTCGTCAGATTCATCCG	
OCN	forward: TATGGCACCACCGTTTAGGG	123 bp
	reverse: CTGTGCCGTCCATACTTTCG	

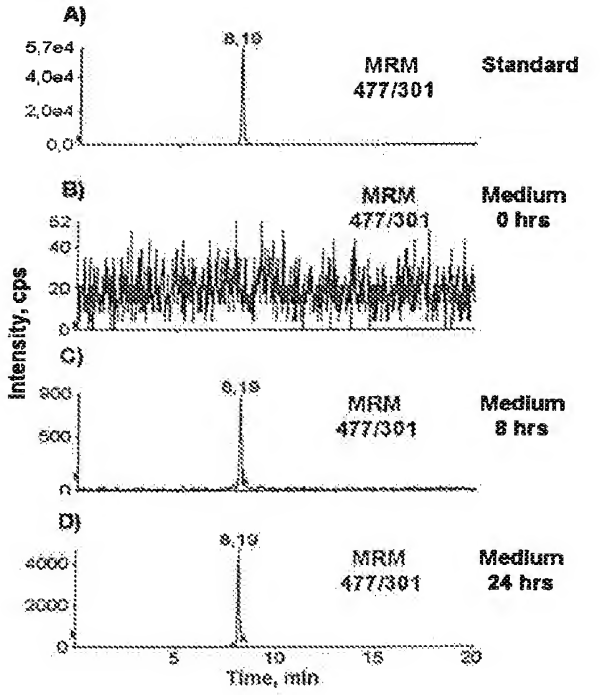

Figure 1. MRM trace chromatograms at hesperetin 7-*O*-glucuronide transition (477/301). (A) standard of hesperetin-7-*O*-glucuronide; (B) medium after 0 h of cell exposure to hesperetin; (C) medium after 8 h of cell exposure to hesperetin; (D) medium after 24 h of cell exposure to hesperetin.

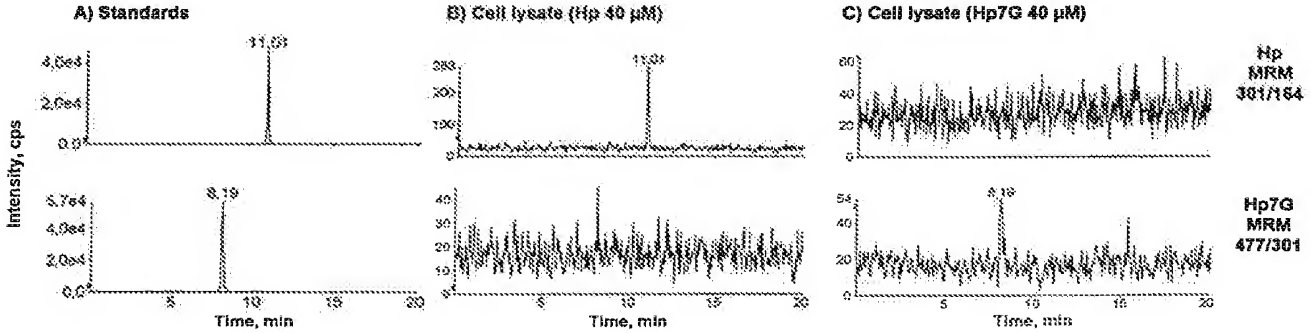

Figure 2. MRM trace chromatograms at hesperetin (301/164) and hesperetin-7-*O*-glucuronide (477/301) transitions from (A) standards; (B) cell lysate after 24 h of exposure to 40 μM Hp; and (C) cell lysate after 24 h of exposure to 40 μM Hp7G.

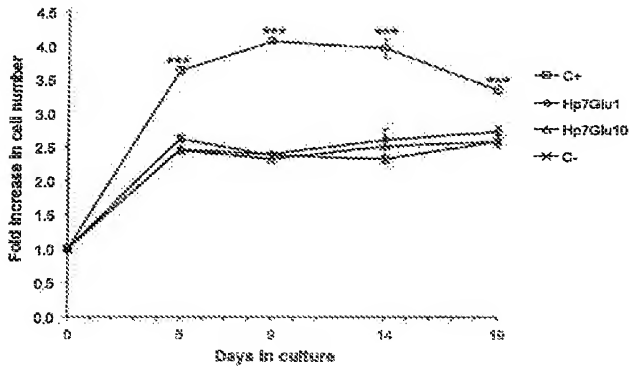

Figure 3. Proliferation of primary osteoblasts cultured in minimal medium (C−; ×), supplemented with 1 μM (Hp7G1; ◇) or 10 μM (Hp7G10; △) hesperetin 7-O-glucuronide, or in optimized medium (C+; □) after 0, 5, 9, 14, and 19 days of treatment. Fold increase in cell number was calculated relative to the initial cell number at day 0. Results are expressed as mean ± SEM. ***$p < 0.001$ vs C−, Hp7G1, and Hp7G10.

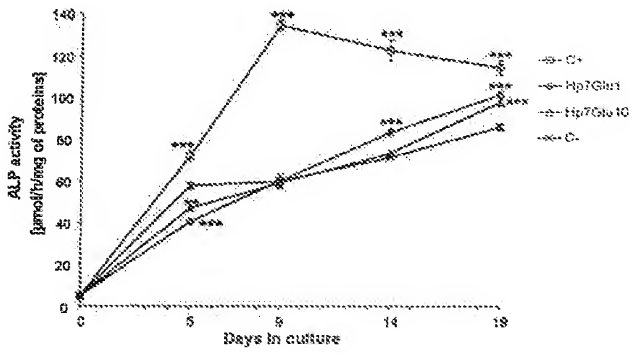

Figure 4. ALP activity of primary osteoblasts cultured in minimal medium (C−; ×), supplemented with 1 μM (Hp7G1; ◇) or 10 μM (Hp7G10; △) hesperetin 7-O-glucuronide, or in optimized medium (C+; □) after 0, 5, 9, 14, and 19 days of treatment. Results are expressed as mean ± SEM. **$p < 0.01$, ***$p < 0.001$ vs C−.

the absence of cells (0.34%), but the extent of hydrolysis was clearly lower than that in the presence of cells. Furthermore, traces of Hp7G were detected in the cell lysate after 24 h-exposure (Figure 2C), even though the concentration was below our quantification limit. Hp was not detected in the cell lysate. Our data thus suggest a very limited but existing penetration of Hp7G in primary rat osteoblasts or interaction of Hp7G with the membrane of osteoblasts.

Cell Proliferation. Impact of Hp7G on cell proliferation on days 0, 5, 9, 14, and 19 was assessed (Figure 3). As expected, increased proliferation was observed until day 5 and remained unchanged after this time in C+ conditions. While a significantly higher proliferation rate was observed in this condition compared to that in the others ($p < 0.001$), Hp7G did not influence proliferation.

Osteoblast Differentiation (ALP Activity). Osteoblast differentiation was assessed kinetically by measuring ALP activity in cells treated for 19 days.

In osteoblasts treated with ascorbic acid and β-glycerophosphate (C+), ALP activity (Figure 4) was significantly increased compared to that in minimal medium (C−) from day 5 up to day 19 ($p < 0.001$). Hp7G at 1 μM (Hp7G1) and 10 μM (Hp7G10) at day 5 decreased ALP activity when compared to C− ($p < 0.01$). However, when Hp7G was added at 1 μM, a significant increase of ALP activity on days 14 and 19 was observed (D14, +16.6%; D19, +18%; $p < 0.001$ vs C−), while only a significant increase was noted on day 19 with the higher dose (D19, +14%; $p < 0.001$ vs C−) (Figure 4).

Gene Expression (Real-Time PCR). The changes in gene expression were considered significant when 20% up (1.20-fold)- or down (1.20-fold)-regulation was obtained, compared to that of C− (value = 1.00).

Runx2 and Osterix Expression. While Runx2 expression was significantly decreased in C+ and Hp7G10 conditions after 24 h of exposure, an increased Runx2 messenger level was measured after 48 h, whatever the treatment (C+, 1.94-fold; Hp7G1, 2.66-fold; Hp7G10, 2.45-fold; $p < 0.05$ vs C−) (Figure 5A). Concerning Osterix, no effect from the treatments was observed after 24 h of culture. However, a decreased mRNA level was reported in C+ conditions (1.61-fold down-regulated; $p < 0.05$ vs C−), while Hp7G at both doses was able to up-regulate Osterix expression after 48 h of exposure (Hp7G1, 1.32-fold; Hp7G10, 1.40-fold; $p < 0.05$ vs C−) (Figure 5A).

OPG and RANKL Expression. Expression of OPG was significantly down-regulated in C+ medium at both times of treatment (24 h, 1.96-fold; 48 h, 1.33-fold; $p < 0.05$ vs C−). The OPG transcript level remained unchanged after Hp7G treatment. Concerning RANKL, after 24 h of treatment, the mRNA level remained unchanged in C+ conditions and was decreased only by Hp7G10 (1.25-fold; $p < 0.05$ vs C−). However, after 48 h of treatment, the decrease was observed in every condition at the same rate, even in C+ medium (2.00-fold; $p < 0.05$ vs C−) (Figure 5B).

Noggin, BMP2, and BMP4 expression. The expression of Noggin was strongly down-regulated in C+ medium whatever the time of exposure (24 h, 3.56-fold; 48 h, 15.60-fold; $p < 0.05$ vs C−). Hp7G, at both doses, was also able to significantly decrease Noggin mRNA level after 24 h (Hp7G1, 1.23-fold; Hp7G10, 1.27-fold; $p < 0.05$ vs C−) and 48 h of treatment (Hp7G1, 1.61-fold; Hp7G10, 1.70-fold; $p < 0.05$ vs C−) (Table 2).

Regarding BMP2 and BMP4, only BMP4 mRNA level after 24 h of treatment was significantly up-regulated in C+ medium (1.47-fold; $p < 0.05$ vs C−). After 24 h of exposure, BMP2 and BMP4 expression was not affected by Hp7G treatment, while after 48 h, a decreased BMP2 messenger level was measured for Hp7G1 (1.45-fold down-regulated; $p < 0.05$ vs C−) (Table 2).

Smad1 and Smad5 Expression. Expression of both genes was down-regulated in C+ medium ($p < 0.05$ vs C−). Smad1 transcript level was not changed by Hp7G treatment, while Hp7G at both doses down-regulated Smad5 expression after 24 h (1.23-fold; $p < 0.05$ vs C−), an increase was observed after 48 h of exposure (Table 2).

c-Jun and c-fos Expression. No significant difference in c-Jun expression was observed, whatever treatment and time of exposure. Regarding c-fos expression, only Hp7G1 was able to decrease the mRNA level after 24 h of treatment (1.23-fold; $p < 0.05$ vs C−) (Table 2).

ALP, OPN, and OCN Expression. ALP expression was not affected after 24 h of treatment. However, after 48 h of exposure, expression of ALP was upregulated in all conditions (C+, 1.30-fold; Hp7G1, 1.45-fold; Hp7G10, 1.39-fold; $p < 0.05$ vs C−) (Table 2).

In the C+ medium, while a significant decrease of OPN expression was observed at both times, OCN expression was strongly upregulated (24 h, 2.20-fold; 48 h, 9.45-fold; $p < 0.05$ vs C−). Hp7G did not have any influence on OPN expression whatever the dose and time of exposure. OCN expression was significantly upregulated in Hp7G10 (1.31-fold; $p < 0.05$ vs C−) after 48 h of treatment (Table 2).

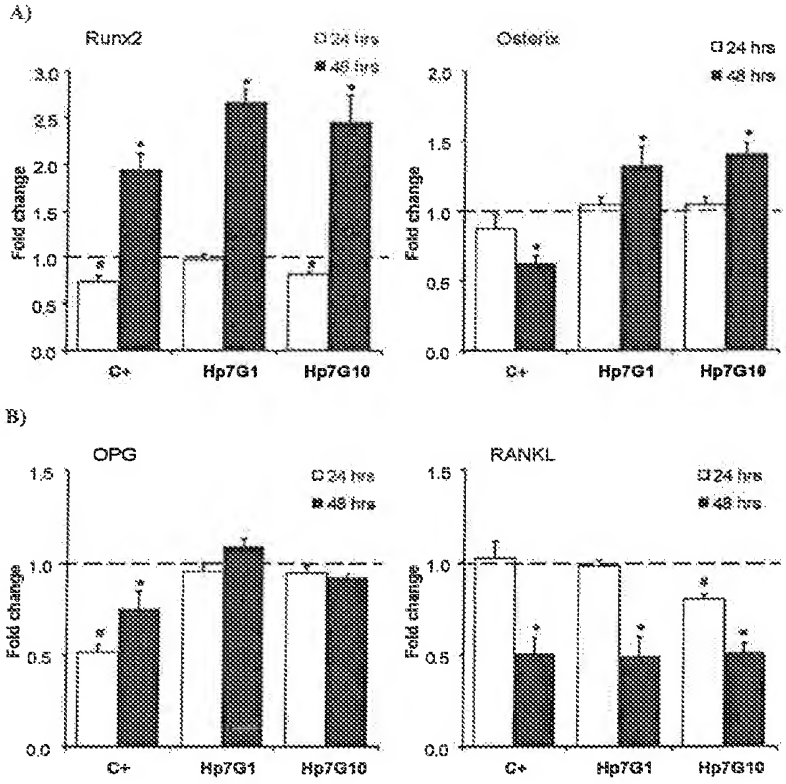

Figure 5. Gene expression of (A) Runx2 and Osterix (B) OPG and RANKL in primary osteoblasts cultured in minimal medium (C−), supplemented with 1 μM (Hp7G1) or 10 μM (Hp7G10) hesperetin 7-*O*-glucuronide, or in optimized medium (C+). Results are presented as fold change compared to C− (dashed line) after 24 and 48 h of exposure. Results are expressed as mean ± SEM. $^{\#}p < 0.05$ vs C− 24 h; $^{*}p < 0.05$ vs C− 48 h.

Table 2. Expression of Osteoblast-Related Genes[a]

gene	time of exposure	fold change C+	Hp7G1	Hp7G10
Noggin	24 h	0.28 ± 0.02#	0.81 ± 0.06#	0.78 ± 0.05#
	48 h	0.06 ± 0.01*	0.62 ± 0.05*	0.59 ± 0.11*
BMP2	24 h	1.23 ± 0.22	0.97 ± 0.08	0.92 ± 0.04
	48 h	1.24 ± 0.10	0.69 ± 0.08*	0.97 ± 0.03
BMP4	24 h	1.47 ± 0.07#	0.96 ± 0.06	0.99 ± 0.08
	48 h	1.00 ± 0.05	1.14 ± 0.14	0.86 ± 0.05
Smad1	24 h	0.76 ± 0.06#	0.95 ± 0.02	1.00 ± 0.02
	48 h	0.69 ± 0.02*	0.91 ± 0.02	0.83 ± 0.06
Smad5	24 h	0.72 ± 0.09#	0.81 ± 0.03#	0.81 ± 0.02#
	48 h	0.94 ± 0.03	1.45 ± 0.13*	1.17 ± 0.06
c-Jun	24 h	1.22 ± 0.17	0.95 ± 0.03	0.98 ± 0.04
	48 h	0.84 ± 0.17	0.96 ± 0.05	1.00 ± 0.14
c-fos	24 h	1.17 ± 0.21	0.81 ± 0.01#	0.86 ± 0.05
	48 h	0.91 ± 0.07	0.97 ± 0.03	0.91 ± 0.02
ALP	24 h	0.93 ± 0.06	0.85 ± 0.02	0.89 ± 0.06
	48 h	1.27 ± 0.08*	1.56 ± 0.09*	1.39 ± 1.39*
OPN	24 h	0.76 ± 0.09#	0.91 ± 0.05	0.96 ± 0.02
	48 h	0.68 ± 0.02*	1.00 ± 0.05	0.95 ± 0.08
OCN	24 h	2.20 ± 0.15#	1.00 ± 0.17	0.91 ± 0.06
	48 h	9.45 ± 0.40*	1.40 ± 0.42	1.31 ± 0.10*

[a] Primary osteoblasts cultured in minimal medium (C−), supplemented with 1 μM (Hp7G1) or 10 μM (Hp7G10) hesperetin 7-*O*-glucuronide or in optimized medium (C+) after 24 h and 48 h of exposure. Results are presented as fold change compared to C− (value = 1.00) after 24 or 48 h of exposure. Results are expressed as mean ± SEM. $^{\#}p < 0.05$ vs C− 24 h. $^{*}p < 0.05$ vs C− 48 h.

Effect of Hp7G on the Phosphorylation of Smad1/5/8 and ERK1/2 Proteins. Phosphorylation of Smad1/5/8 and ERK1/2 proteins was assessed by Western blotting on cell lysates from cells treated for 24 and 48 h (Figure 6A and B). The antibodies anti-Smad1/5/8 and antiphospho-Smad1/5/8 used in the Western blot analysis can recognize three Smad proteins, 1, 5, and 8. Because of the specificity of antibodies as well as the expression of proteins, two or three bands may be visible.

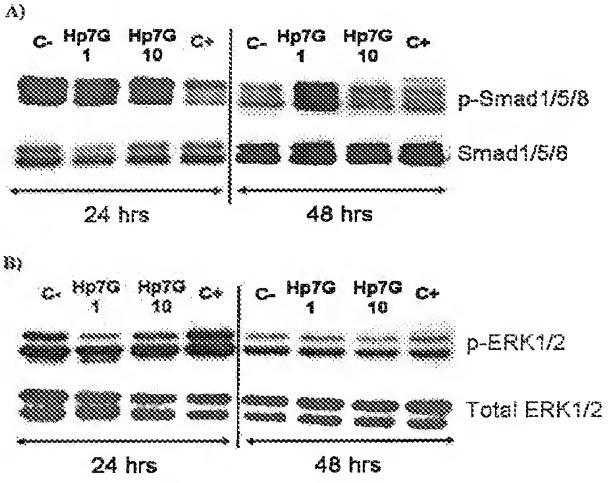

Figure 6. Phosphorylation of (A) Smad1/5/8 proteins and (B) ERK1/2 proteins in primary osteoblasts cultured in minimal medium (C−), supplemented with 1 μM (Hp7G1) or 10 μM (Hp7G10) hesperetin 7-*O*-glucuronide, or in optimized medium (C+) after 24 and 48 h of exposure.

The observations reported here are qualitative and not quantitative.

C+ and Hp7G at both doses could decrease the phosphorylation of Smad1/5/8 after 24 h of treatment; the strongest effect was obtained with Hp7G1. On the contrary, after 48 h of exposure, phosphorylation of Smad1/5/8 seemed to be enhanced by Hp7G1 (**Figure 6A**).

Concerning ERK1/2, phosphorylation was decreased in Hp7G conditions compared to that in C−, while no difference between C− and C+ was detected after 24 h of exposure. Phosphorylation of ERK1/2 after 48 h of treatment was lower than that after 24 h of exposure, and moreover, no differences between conditions could be detected (**Figure 6B**).

DISCUSSION

It has been previously demonstrated that hesperetin (aglycone form of hesperidin) can influence bone formation via stimulation of osteoblast differentiation mainly through the BMP pathway (*7*). In this study, we focused on the potential effects of hesperetin-7-*O*-glucuronide, its main metabolite, on the same experimental model. Indeed, the circulating forms may possess different biological properties within cells and tissues compared to those of polyphenol aglycones (*24*).

Cellular Uptake. Activation of cell signaling can occur via different ways including an interaction of a compound with a receptor on the cell surface and/or by interaction with extracellular proteins (*9*). However, some nutrients which are able to enter cells through a transporter mediated process or by passive diffusion may directly interact with transcription factors, thus affecting the target gene expression (*25*). It has been shown that aglycone forms of flavonoids can cross cell membranes by passive diffusion, whereas conjugates need active transport (*9*, *26*). In primary rat osteoblasts, we observed that the cellular uptake of Hp was definitely more efficient than that of Hp7G, which was too limited to be unambiguously demonstrated in our conditions. We only observed (i) a small increase of Hp7G hydrolysis in the medium when cells were present compared to when Hp7G was incubated in cell-free medium and (ii) traces of Hp7G in the cell extract after 24 h of exposure to glucuronide, which may also reflect binding to cell membranes. Primary cell osteoblasts may lack efficient transporters to facilitate the uptake of flavonoid glucuronides. However, these cells were shown to export Hp7G in the medium after Hp exposure (**Figure 1**), which shows that primary osteoblasts are able to glucuronide Hp as shown for Caco-2 cells (*27*, *28*) and fibroblasts (*11*), and possess transporters to efficiently export flavonoid glucuronides. Our results thus suggest a very transient presence of Hp7G inside the primary rat osteoblasts after either Hp or Hp7G exposure. This transient presence was nevertheless associated with a positive effect on cell differentiation when osteoblasts were exposed to glucuronide.

Effect of Hp7G on Osteoblast Proliferation and Differentiation. This study has assessed the impact of a hesperetin conjugate on osteoblast cells at nutritional and physiological concentrations (1 and 10 μM). The choice of nutritional doses led to significant cellular responses but were quite small.

In our experimental conditions, Hp7G, similarly to its aglycone form (*7*, *29*) and to other polyphenols (*30*−*32*), did not affect osteoblast proliferation (**Figure 3**) but was able to influence osteoblast differentiation (**Figure 4**). Even if Hp7G decreased ALP activity on day 5, which could reflect a faster commitment of these cells compared to the cells cultivated in minimal medium (*33*), the final effect of treatment is crucial to interpret results. Hp7G at 1 μM (on days 14 and 19) and 10 μM (on day 19) increased ALP activity, which can also play a role in osteoblast mineralization probably by a release of the phosphate necessary for calcium nodule formation (*34*, *35*). Surprisingly, Hp7G1 was more efficient than Hp7G10, whereas hesperetin at the 10 μM dose was more efficient than 1 μM (*7*). Moreover, Hp7G1 increased ALP activity from day 14, while Hp7G10 was only at day 19. Again, this was inversed when cells were exposed to hesperetin (*7*). In other studies, similar dose-dependent patterns of ALP activity in osteoblasts exposed to different agiycone compounds were reported (*30*, *36*); however, data with their corresponding metabolites are still lacking. This is probably because conjugated molecules are not commercialized (*24*). However, the glucuronide form of hesperetin was more efficient than the aglycone parent form in stimulating osteoblast differentiation as previously assessed (*7*). The same observation was reported for quercetin and its glucuronide in HUVEC cells (*37*). This kind of experiment supports the fact that conjugates can share physiological bioactivities, even if they are poorly or not absorbed by cells (*28*).

Possible Signaling Pathways Involved in Hp7G Action. Gene expression was analyzed after 24 and 48 h of exposure. In our experimental conditions, a stronger effect on gene expression was observed after 48 h of treatment (**Figure 5** and **Table 2**), suggesting that the duration of exposure may influence the gene response. For almost all genes evaluated, the level of mRNA appeared to be similar for 1 and 10 μM Hp7G. It can be hypothesized that the effective dose of Hp7G to modulate bone related genes in primary osteoblasts is 1 μM, this being consistent with ALP findings (**Figure 3**). However, this does not exclude the higher efficacy of a lower dose of glucuronide and should therefore be evaluated.

In our experimental conditions, ALP and OCN mRNA levels were increased after 48 h of Hp7G treatment (**Table 2**). Expression of these genes may be regulated by Runx2 (*38*). Moreover, Hp7G was able to upregulate the expression of not only Runx2 but also Osterix (**Figure 5A**), which are two main transcription factors related to osteoblasts (*14*) and are involved in BMP (*39*) and MAPK signaling (*15*, *40*). Similar results were obtained for some polyphenol aglycones such as hesperetin (*7*), resveratrol (*41*), and epigallocatechin gallate (EGCG) (*42*).

Mechanisms of interaction with Runx2 are complex, including binding of components such as AP-1 factors and Smad proteins to DNA regions in target gene promoters. Regarding Smad phosphorylation, Hp7G1 seemed to increase the phosphorylation of the Smad1/5/8 complex after 48 h of exposure (**Figure 6A**). This result is consistent with those of several authors who have demonstrated the possible phosphorylation of the Smad1/5/8 complex in osteoblasts treated with some polyphenols such as myricetin (*30*) and coumarin derivates (*31*, *43*). This suggests that the BMP pathway via the activation of Smad1/5/8 may be implicated in Hp7G action even if BMP2 and BMP4 gene expression was not increased (**Table 2**), contrary to previous findings concerning some polyphenols (*30*, *31*, *36*, *43*, *44*) including hesperetin (*7*). This could be due to the fact that aglycones and not conjugates were used. However, in this study, the hesperetin metabolite decreased expression of Noggin, one of the osteoblast secreted proteins which can limit the level of BMP signals (*45*), supporting the hypothesized interaction of hesperetin glucuronide with the BMP pathway.

The effects of Hp7G on c-Jun and c-fos (components of complex AP-1), and on ERK1/2, both implicated in the MAPK cascade, were assessed. In our experimental design, the glucuronide could only slightly decrease c-fos gene expression and was able to decrease the phosphorylation of ERK1/2 after 24 h of exposure, while no effect after 48 h was reported (**Figure 6B**). On the contrary, it has been shown that some coumarin aglycones at 10 μM were able to stimulate the phosphorylation of ERK1/2 in primary rat osteoblasts after 12 h of exposure (*31*). However, the

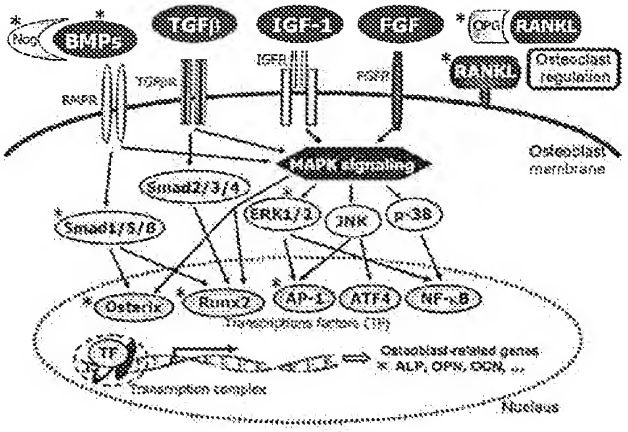

Figure 7. Signaling pathways implicated in the regulation of osteoblast differentiation. Asterisks (*) mark the obtained effect of hesperetin-7-*O*-glucuronide (Hp7G) on gene expression involved in osteoblast differentiation, in our experimental conditions (see Table 2 and Figure 5 for details).

phosphorylation of ERK1/2 in MC3T3-E1 osteoblast exposure to EGCG (10−30 μM) for 60 min remained unchanged compared to that of nontreated cells (*46*). Regarding our results, it is difficult to draw a clear conclusion about an interaction of Hp7G with MAPK signaling. It could be possible that aglycone forms can activate MAPK signaling including JNK, ERK1/2, and p-38 MAPK because they activate some of the phase II drug-metabolizing enzymes which are responsible for their conjugation (*47*). In the case of glucuronides, these enzymes are not necessary. This could explain why Hp7G failed to activate MAPK/ERK signaling. Thus, different signaling pathways may be activated compared to those in aglycones.

A further important outcome of this study is the finding that the hesperetin conjugate is able to decrease the gene expression of RANKL while at the same time not change OPG expression (Figure 5B). These results suggest that Hp7G may be able to limit osteoclast activation, as previously shown for daidzein and genistein (*48*).

Conclusions. Our data demonstrated that hesperetin glucuronide is able to affect osteoblast differentiation at nutritional and physiological doses. Indeed, Hp7G may act on osteoblasts mainly through Runx2 and Osterix activation by molecular mechanisms not well identified (Figure 7). It is possible that these transcription factors could interact with the BMP cascade and/or MAPK signaling. However, further mechanistic studies are necessary to confirm this hypothesis.

ABBREVIATIONS USED

ALP, alkaline phosphatase; AP-1, activator protein 1; BMP, bone morphogenetic protein; ERK, extracellular signal-regulated kinase; Hp, hesperetin; Hp7G, hesperetin-7-*O*-glucuronide; JNK, c-Jun N-terminal kinase; MAPK, mitogen-activated protein kinase; OCN, osteocalcin; OPG, osteoprotegerin; OPN, osteopontin; RANKL, receptor activator of nuclear factor-kappaB (RANK) ligand.

LITERATURE CITED

(1) Manach, C.; Morand, C.; Gil-Izquierdo, A.; Bouteloup-Demange, C.; Remesy, C. Bioavailability in humans of the flavanones hesperidin and narirutin after the ingestion of two doses of orange juice. *Eur. J. Clin. Nutr.* **2003**, *57*, 235–242.

(2) Matsumoto, H.; Ikoma, Y.; Sugiura, M.; Yano, M.; Hasegawa, Y. Identification and quantification of the conjugated metabolites derived from orally administered hesperidin in rat plasma. *J. Agric. Food Chem.* **2004**, *52*, 6653–9.

(3) Chiba, H.; Uehara, M.; Wu, J.; Wang, X. X.; Masuyama, R.; Suzuki, K.; Kanazawa, K.; Ishimi, Y. Hesperidin, a citrus flavonoid, inhibits bone loss and decreases serum and hepatic lipids in ovariectomized mice. *J. Nutr.* **2003**, *133*, 1892–1897.

(4) Horcajada, M. N.; Habauzit, V.; Trzeciakiewicz, A.; Morand, C.; Gil-Izquierdo, A.; Mardon, J.; Lebecque, P.; Davicco, M. J.; Chee, W. S.; Coxam, V.; Offord, E. Hesperidin inhibits ovariectomized-induced osteopenia and shows differential effects on bone mass and strength in young and adult intact rats. *J. Appl. Physiol.* **2008**, *104*, 648–654.

(5) Garg, A.; Garg, S.; Zaneveld, L. J. D.; Singla, A. K. Chemistry and pharmacology of the citrus bioflavonoid hesperidin. *Phytother Res.* **2001**, *15*, 655–669.

(6) Deyhim, F.; Garica, K.; Lopez, E.; Gonzalez, J.; Ino, S.; Garcia, M.; Patil, B. S. Citrus juice modulates bone strength in male senescent rat model of osteoporosis. *Nutrition* **2006**, *22*, 559–563.

(7) Trzeciakiewicz, A.; Habauzit, V.; Mercier, S.; Lebecque, P.; Davicco, M. J.; Demigne, C.; Horcajada, M. N. Hesperetin stimulates differentiation of primary rat osteoblasts involving the BMP signalling pathway. *J. Nutr. Biochem.* [Online early access]. DOI: 10.1016/j.nutbio.2009.01.017.

(8) Xu, C.; Li, C. Y.; Kong, A. N. Induction of phase I, II and III drug metabolism/transport by xenobiotics. *Arch. Pharm. Res.* **2005**, *28*, 249–68.

(9) Williamson, G.; Barron, D.; Shimoi, K.; Terao, J. In vitro biological properties of flavonoid conjugates found in vivo. *Free Radical Res.* **2005**, *39*, 457–469.

(10) Kim, D. S.; Takai, H.; Arai, M.; Araki, S.; Mezawa, M.; Kawai, Y.; Murota, K.; Terao, J.; Ogata, Y. Effects of quercetin and quercetin 3-glucuronide on the expression of bone sialoprotein gene. *J. Cell Biochem.* **2007**, *101*, 790–800.

(11) Proteggente, A. R.; Basu-Modak, S.; Kuhnle, G.; Gordon, M. J.; Youdim, K.; Tyrrell, R.; Rice-Evans, C. A. Hesperetin glucuronide, a photoprotective agent arising from flavonoid metabolism in human skin fibroblasts. *Photochem. Photobiol.* **2003**, *78*, 256–261.

(12) Vauzour, D.; Vafeiadou, K.; Rice-Evans, C.; Williams, R. J.; Spencer, J. P. E. Activation of pro-survival Akt and ERK1/2 signalling pathways underlie the anti-apoptotic effects of flavanones in cortical neurons. *J. Neurochem.* **2007**, *103*, 1355–1367.

(13) Trzeciakiewicz, A.; Habauzit, V.; Horcajada, M. N. When nutrition interacts with osteoblast function: molecular mechanisms of polyphenols. *Nutr. Res. Rev.* **2009**, 1–15.

(14) Marie, P. J. Transcription factors controlling osteoblastogenesis. *Arch. Biochem. Biophys.* **2008**, *473*, 98–105.

(15) Franceschi, R. T.; Xiao, G. Z. Regulation of the osteoblast-specific transcription factor, runx2: Responsiveness to multiple signal transduction pathways. *J. Cell Biochem.* **2003**, *88*, 446–454.

(16) Miyazono, K.; Maeda, S.; Imamura, T. BMP receptor signaling. Transcriptional targets, regulation of signals, and signaling cross-talk. *Cytokine Growth Factor Rev.* **2005**, *16*, 251–63.

(17) De Wilde, A.; Lieberherr, M.; Colin, C.; Pointillart, A. A low dose of daidzein acts as an ERbeta-selective agonist in trabecular osteoblasts of young female piglets. *J. Cell Physiol.* **2004**, *200*, 253–262.

(18) Pang, J. L.; Ricupero, D. A.; Huang, S.; Fatma, N.; Singh, D. P.; Romero, J. R.; Chattopadhyay, N. Differential activity of kaempferol and quercetin in attenuating tumor necrosis factor receptor family signaling in bone cells. *Biochem. Pharmacol.* **2006**, *71*, 818–26.

(19) Boyce, B. F.; Xing, L. P. Functions of RANKL/RANK/OPG in bone modeling and remodeling. *Arch. Biochem. Biophys.* **2008**, *473*, 139–146.

(20) Boumendjel, A.; Blanc, M.; Williamson, G.; Barron, D. Efficient synthesis of flavanone glucuronides. *J. Agric. Food Chem.* **2009**, *57*, 7264–7267.

(21) Declercq, H.; Van den Vreken, N.; De Maeyer, E.; Verbeeck, R.; Schacht, E.; De Ridder, L.; Cornelissen, M. Isolation, proliferation and differentiation of osteoblastic cells to study cell/biomaterial interactions: comparison of different isolation techniques and source. *Biomaterials* **2004**, *25*, 757–768.

(22) Sabokbar, A.; Millett, P. J.; Myer, B.; Rushton, N. A rapid, quantitative assay for measuring alkaline-phosphatase activity in osteoblastic cells in-vitro. *Bone Miner.* **1994**, *27*, 57–67.

(23) Livak, K. J.; Schmittgen, T. D. Analysis of relative gene expression data using real-time quantitative PCR and the 2(-delta delta C(T)) method. *Methods* **2001**, *25*, 402–8.

(24) Kroon, P. A.; Clifford, M. N.; Crozier, A.; Day, A. J.; Donovan, J. L.; Manach, C.; Williamson, G. How should we assess the effects of exposure to dietary polyphenols in vitro? *Am. J. Clin. Nutr.* **2004**, *80*, 15–21.

(25) Muller, M.; Kersten, S. Nutrigenomics: goals and strategies. *Nat. Rev. Genet.* **2003**, *4*, 315–22.

(26) Morris, M. E.; Zhang, S. Flavonoid-drug interactions: effects of flavonoids on ABC transporters. *Life Sci.* **2006**, *78*, 2116–30.

(27) Brand, W.; van der Wel, P. A. I.; Rein, M. J.; Barron, D.; Williamson, G.; van Bladeren, P. J.; Rietjens, I. Metabolism and transport of the citrus flavonoid hesperetin in Caco-2 cell monolayers. *Drug Metab. Dispos.* **2008**, *36*, 1794–1802.

(28) Serra, H.; Mendes, T.; Bronze, M. R.; Simplicio, A. L. Prediction of intestinal absorption and metabolism of pharmacologically active flavones and flavanones. *Bioorg. Med. Chem.* **2008**, *16*, 4009–4018.

(29) Choi, E. M.; Kim, Y. H. Hesperetin attenuates the highly reducing sugar-triggered inhibition of osteoblast differentiation. *Cell Biol. Toxicol.* **2008**, *24*, 225–31.

(30) Hsu, Y. L.; Chang, J. K.; Tsai, C. H.; Chien, T. T. C.; Kuo, P. L. Myricetin induces human osteoblast differentiation through bone morphogenetic protein-2/p38 mitogen-activated protein kinase pathway. *Biochem. Pharmacol.* **2007**, *73*, 504–514.

(31) Tang, C. H.; Yang, R. S.; Chien, M. Y.; Chen, C. C.; Fu, W. M. Enhancement of bone morphogenetic protein-2 expression and bone formation by coumarin derivatives via p38 and ERK-dependent pathway in osteoblasts. *Eur. J. Pharmacol.* **2008**, *579*, 40–49.

(32) Zhao, J.; Ohba, S.; Shinkai, M.; Chung, U. I.; Nagamune, T. Icariin induces osteogenic differentiation in vitro in a BMP- and Runx2-dependent manner. *Biochem. Biophys. Res. Commun.* **2008**, *369*, 444–448.

(33) Aubin, J. E. Advances in the osteoblast lineage. *Biochem. Cell Biol.* **1998**, *76*, 899–910.

(34) Siffert, R. S. The role of alkaline phosphatase in osteogenesis. *J. Exp. Med.* **1951**, *93*, 415–426.

(35) Sugawara, Y.; Suzuki, K.; Koshikawa, M.; Ando, M.; Iida, J. Necessity of enzymatic activity of alkaline phosphatase for mineralization of osteoblastic cells. *Jpn. J. Pharmacol.* **2002**, *88*, 262–269.

(36) Chang, J. K.; Hsu, Y. L.; Teng, L. C.; Kuo, P. L. Piceatannol stimulates osteoblast differentiation that may be mediated by increased bone morphogenetic protein-2 production. *Eur. J. Pharmacol.* **2006**, *551* (1−3), 1–9.

(37) Tribolo, S.; Lodib, F.; Connor, C.; Suri, S.; Wilson, V. G.; Taylor, M. A.; Needs, P. W.; Kroon, P. A.; Hughes, D. A. Comparative effects of quercetin and its predominant human metabolites on adhesion molecule expression in activated human vascular endothelial cells. *Atherosclerosis* **2008**, *197*, 50–56.

(38) Ducy, P.; Zhang, R.; Geoffroy, V.; Ridall, A. L.; Karsenty, G. Osf2/Cbfa1: a transcriptional activator of osteoblast differentiation. *Cell* **1997**, *89*, 747–54.

(39) Yamaguchi, A.; Komori, T.; Suda, T. Regulation of osteoblast differentiation mediated by bone morphogenetic proteins, hedgehogs, and Cbfa1. *Endocr. Rev.* **2000**, *21*, 393–411.

(40) Celil, A. B.; Hollinger, J. O.; Campbell, P. G. Osx transcriptional regulation is mediated by additional pathways to BMP2/Smad signaling. *J. Cell Biochem.* **2005**, *95*, 518–528.

(41) Dai, Z.; Li, Y.; Quarles, L. D.; Song, T.; Pan, W.; Zhou, H.; Xiao, Z. Resveratrol enhances proliferation and osteoblastic differentiation in human mesenchymal stem cells via ER-dependent ERK1/2 activation. *Phytomedicine* **2007**, *14*, 806–814.

(42) Chen, C. H.; Ho, M. L.; Chang, J. K.; Hung, S. H.; Wang, G. J. Green tea catechin enhances osteogenesis in a bone marrow mesenchymal stem cell line. *Osteoporosis Int.* **2005**, *16*, 2039–2045.

(43) Kuo, P.-L.; Hsu, Y.-L.; Chang, C.-H.; Chang, J.-K. Osthole-mediated cell differentiation through bone morphogenetic protein-2/p38 and extracellular signal-regulated kinase 1/2 pathway in human osteoblast cells. *J. Pharmacol. Exp. Ther.* **2005**, *314*, 1290–1299.

(44) Zhao, J.; Ohba, S.; Shinkai, M.; Chung, U. I.; Nagamune, T. Icariin induces osteogenic differentiation in vitro in a BMP- and Runx2-dependent manner. *Biochem. Biophys. Res. Commun.* **2008**, *369*, 444–8.

(45) Groppe, J.; Greenwald, J.; Wiater, E.; Rodriguez-Leon, I.; Economides, A. N.; Kwiatkowski, W.; Affolter, M.; Vale, W. W.; Belmonte, J. C. I.; Choe, S. Structural basis of BMP signalling inhibition by the cystine knot protein Noggin. *Nature* **2002**, *420*, 636–642.

(46) Hayashi, K.; Takai, S.; Matsushima-Nishiwaki, R.; Hanai, Y.; Kato, K.; Tokuda, H.; Kozawa, O. (−)-Epigallocatechin gallate reduces transforming growth factor beta-stimulated HSP27 induction through the suppression of stress-activated protein kinase/c-Jun N-terminal kinase in osteoblasts. *Life Sci.* **2008**, *82*, 1012–1017.

(47) Kong, A. N.; Owuor, E.; Yu, R.; Hebbar, V.; Chen, C.; Hu, R.; Mandlekar, S. Induction of xenobiotic enzymes by the MAP kinase pathway and the antioxidant or electrophile response element (ARE/EpRE). *Drug Metab. Rev.* **2001**, *33*, 255–71.

(48) Chen, X. W.; Garner, S. C.; Anderson, J. J. Isoflavones regulate interleukin-6 and osteoprotegerin synthesis during osteoblast cell differentiation via an estrogen-receptor-dependent pathway. *Biochem. Biophys. Res. Commun.* **2002**, *295*, 417–22.

Received for review July 31, 2009. Revised manuscript received November 7, 2009. Accepted November 09, 2009.